Weighted Synthetic Aperture Focusing for Optoacoustic Microscopy with Scanning Illumination and Detection

Héctor Estrada[a], Jake Turner[a,b], Moritz Kneipp[a,b], and Daniel Razansky[a,b]

[a]Institute for Biological and Medical Imaging (IBMI), Helmholtz Center Munich, Germany
[b]School of Medicine and School of Electrical Engineering and Information Technology, Technical University of Munich, Germany

ABSTRACT

Scanning optoacoustic microscopy operates in two distinct regimes optical resolution microscopy relies on a focused illumination and acoustic resolution microscopy that forms images by focusing the received acoustic field. Recently, a number of approaches have been proposed that combine those two modes of operation to create a highly scalable technique that can image at multiple penetration scales by gradually exchanging microscopic optical resolution in superficial tissues with ultrasonic resolution at diffuse (macroscopic) depths. However, scanning microscopy schemes commonly employ acquisition geometries that impede the use of synthetic aperture techniques to achieve meaningful images due to non-stationary illumination patterns and strong non-uniformity of the excitation light field.

Here we present a Weighted Synthetic Aperture Focusing Technique (W-SAFT) as a universal framework that effectively accounts for the non-uniform distribution of both the excitation light field and spatial sensitivity field of the detector. As a result, W-SAFT maintains optical resolution performance at superficial depths while improving the acoustic resolving capacity for deeper tissues. The dynamic range of the optoacoustic data is compressed using a general fluence decay term applied to the W-SAFT operator, allowing a more uniform visualization of the entire imaged volume. Our three-dimensional algorithm makes use of the sample's surface to account for the heterogeneity produced when scanning a finite-size light beam. We tested a GPU implementation of W-SAFT with numerical simulations and showcase its performance on experimental data acquired from targets embedded in tissue mimicking phantoms.

Keywords: optoacoustic microscopy, photoacoustic microscopy, image reconstruction techniques

1. INTRODUCTION

In optoacoustic imaging,[1,2] broadband ultrasonic waves are generated by deposition of nanosecond laser pulses in biological tissue. The resolution and penetration depth are dictated by the overlap between the illumination and the field of view (FOV) of the ultrasound transducer. In particular, scanning optoacoustic microscopy uses moving ultrasound detection and illumination that can be arranged in three main variants (Fig. 1).

In acoustic resolution (AR) optoacoustic microscopy (OAM),[3] a focused ultrasound transducer is used and illumination is usually broad with respect to the transducer's FOV. The AR-OAM approach is successful at imaging many centimeters deep in optically scattering media limited by the properties of the transducer e.g. numerical aperture, bandwidth, sensitivity. The lateral resolution outside the focal area can be restored through methods such as the virtual detector method,[4] synthetic aperture focusing technique (SAFT),[5] and model matrix inversion.[6,7] However, light fluence distribution in the imaged tissue plays a crucial role, particularly when synthetic aperture focusing is applied to datasets acquired with scanning illumination.

On the other hand, in optical resolution (OR) OAM[8–10] an unfocused ultrasound transducer is used and the lateral-resolution is dictated by the beam width of the focused illumination at a given depth. The achievable lateral resolution of the OR method can theoretically be very high, approaching the optical diffraction limit. However, biomedical imaging targets are typically optically scattering, thus after a few hundred micrometers the

Further author information: (Send correspondence to D.R.)
D.R.: E-mail: dr@tum.de

Photons Plus Ultrasound: Imaging and Sensing 2017, edited by Alexander A. Oraevsky, Lihong V. Wang, Proc. of SPIE Vol. 10064, 100642L · © 2017 SPIE · CCC code: 1605-7422/17/$18 · doi: 10.1117/12.2252930

beam becomes diffuse, which limits the effective penetration of the modality to superficial depths.[11] Overall, OR microscopy is capable of achieving greater resolution than AR microscopy, though the latter is the only valid approach for deep-tissue imaging.

Hybrid focus optoacoustic microscopy (HF-OAM) systems, which employ a combination of focused illumination and focused ultrasound detection are being developed.[12,13] These systems aim to provide OR at the tissue surface, gradually converted to an acoustic resolution at depths where the light is diffuse. Here it is similarly necessary that any algorithms employed to restore out-of-focus lateral resolution in the AR regime do not impair the lateral-resolution in the OR regime. Additionally, although computationally fast, SAFT or other existing delay-sum based image reconstruction algorithms do not address the issue of light fluence, as they are based on the assumption of an AR scenario and thus homogeneous illumination.

We present a weighted synthetic aperture focusing technique (W-SAFT) to account for arbitrary scanning fluence in optoacoustic microscopy systems. This algorithm considers the transducer sensitivity, optical beam properties, and optical properties of the imaging target, to give optimal lateral resolution throughout the scanned volume. Additionally, amplitudes are compressed to within a more useful dynamic range preserving the relative strength of the different optical absorbers in the corrected images.

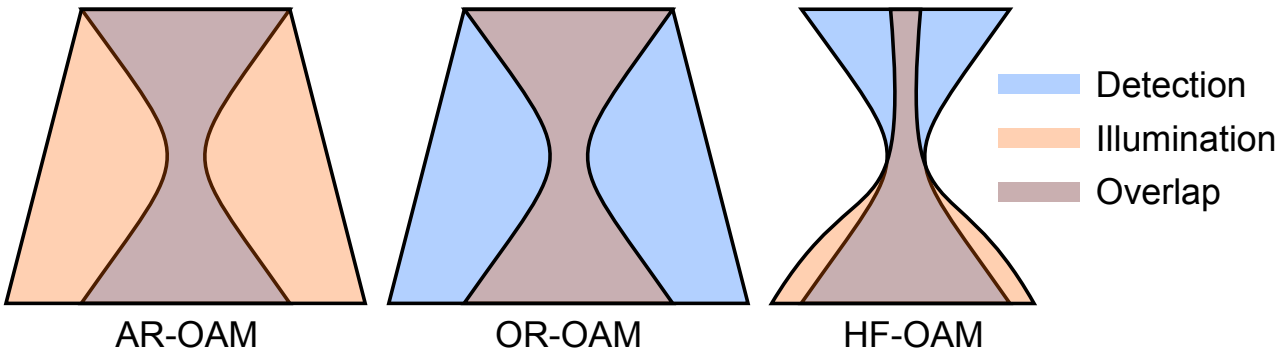

Figure 1. Diagrams showing the different OAM modalities.

2. W-SAFT

In general, summation through equal delay at each transducer position for a data set restores the out-of-focus lateral acoustic resolution. This operation is readily applied to AR-OAM data, however, for OR-OAM, or the OR-to-AR transitional (mesoscopic) regime in HF-OAM, SAFT will laterally blur data in all planes where the fluence is narrower than the lateral FOV of the transducer. To avoid the blurring, we define the limits to the equal delay summation by calculating the overlap between illumination and the transducer's FOV. The overlap depends on the scanning position if the surface of the imaged sample is not flat. One further artifact in the results of SAFT processed data is an amplitude bias for out-of-focus sources. The summation based operation has many more contributions out-of-focus than near-focus. We correct for this artifact calculating a normalization factor which depends on the depth and the summation limits. The fluence correction is performed separately first considering normalize lateral beam spreading normalized through the equal-delay paths and in a second step using a depth-dependent attenuation function, $A(z) = e^{\alpha z}$. As the fluence distribution in HF-OAM is scanning in the lateral plane, it is imperative that correction for $A(z)$ be included in the SAFT operation, and not as a pre- or post-correction step.

One major limitation in the peak-to-peak amplitude equalization of signals from sources in the optically-dictated resolution regime is, intuitively, that as not all possible lateral contributions exist, the superposition necessary for full peak-peak equalization cannot be achieved.

3. METHODS

In the post-processing of the simulated and experimental scans, a PC with 64GB RAM, a 3.2GHz processor (i7 3930, Intel, USA) and a GPU with 2304 cores and 3GB onboard memory (GeForce GTX 780, Nvidia, USA) was used. We simulated a total of 9 microspheres of 60μm in diameter arranged at equal vertical intervals spaced uniformly in a grid through x-y plane (see Fig. 2). The surface of the optically scattering sample was modeled as a dome of concentric rings having uniform depth and the same step size. An additional attenuation-modeling gain of -12 dB/cm was introduced below the scattering surface.

The optoacoustic waveform of the microspheres was calculated using the model developed in[14] and the detection of that pressure by the spherically focused transducer using the program Field-II.[15]

Two phantoms were made with sutures of 50 μm cross-sectional diameter mounted in a cylinder of agar. To test the OR regime we introduced 6 sutures in clear agar, whereas to test the AR regime, 5 sutures were introduced in highly scattering (1% intralipid concentration) agar.

The scans were performed with a fast-scanning HF-OAM system that uses a spherically focused PVDF ultrasound transducer for detection.[16] Illumination (275μJ) was delivered through a multimode fiber with an NA of 0.39 and a core diameter of 600μm (FT600UMT, Thorlabs, DE).

4. RESULTS

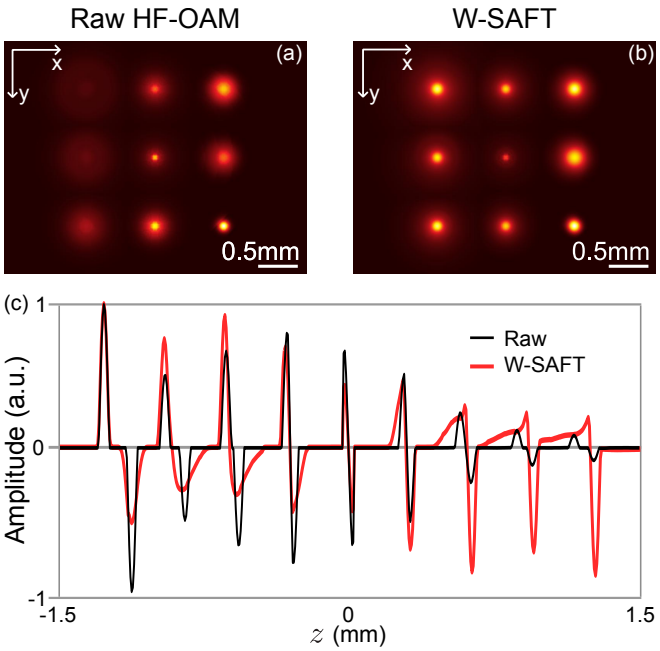

Figure 2. Maximum amplitude projection through z for (a) raw HF-OAM and (b) W-SAFT processed data. (c) Detected pressure at the center of the simulated spheres as a function of depth z. $z = 0$ corresponds to the focus of the transducer.

The results of applying W-SAFT to the simulated data are presented in Fig. 2, demonstrating significant improvement in the out of focus lateral resolution in the AR regime ($z > -0.5$), whilst retaining optically dictated lateral resolution in the OR regime ($z < -0.5$). In Fig. 2(c), a composite time-domain signal shows how in the OR regime the central signal for a sphere will still have temporally-distinct peak amplitudes even after the W-SAFT processing, due to the limited-contribution effects. Furthermore, the relative difference in normalized amplitude between the highest- and lowest-amplitude peak is 56%.

The performance of our method is further confirmed in the experimental results using the agar-suture phantom, as can be seen from Fig. 3. The out-of-focus lateral resolution in AR data is improved, the lateral resolution

in OR data is maintained below a 19% mean decrease and in both cases a high degree of peak-peak amplitude compression is achieved. In the AR case, the advantages of W-SAFT are even more obvious. In the raw data only one suture is readily distinguishable, due to it's proximity to the acoustic focus. Conversely, in the W-SAFT processed data, all sutures are also clearly visible both with respect to their lateral resolution and the very small difference in amplitudes.

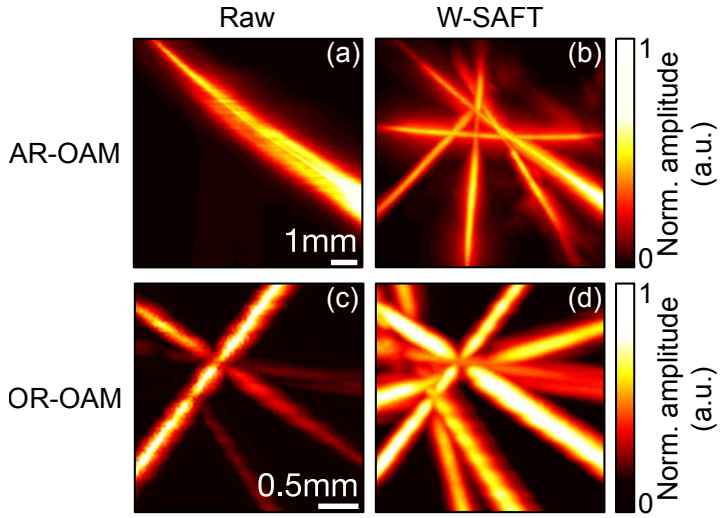

Figure 3. MAPs for experimental AR data ((a) and (b)) and OR data ((c) and (d)).

5. CONCLUSIONS

We developed a Weighted Synthetic Aperture Focusing Technique (W-SAFT) to postprocess the data acquired with scanning optoacoustic microscopy systems in any of its modalities, i.e. AR-OAM, OR-OAM, or HF-OAM. Our framework includes the effect of the transducer's geometry and the moving illumination in three dimensions. Simulations and experimental data of tissue mimicking phantoms show the flexibility and potential of the proposed algorithm.

ACKNOWLEDGMENTS

The research leading to these results has received funding from the European Research Council under grant agreements ERC-2010-StG-260991 and FP7-ITN-2012-317526.

REFERENCES

[1] Ntziachristos, V., "Going deeper than microscopy: the optical imaging frontier in biology," *Nature methods* **7**(8), 603–614 (2010).

[2] Wang, L. V., "Multiscale photoacoustic microscopy and computed tomography," *Nature photonics* **3**(9), 503–509 (2009).

[3] Maslov, K., Zhang, H. F., Hu, S., and Wang, L. V., "Optical-resolution photoacoustic microscopy for in vivo imaging of single capillaries," *Opt. Lett.* **33**, 929–931 (May 2008).

[4] Li, M.-L., Zhang, H. F., Maslov, K., Stoica, G., and Wang, L. V., "Improved in vivo photoacoustic microscopy based on a virtual-detector concept," *Opt. Lett.* **31**, 474–476 (Feb 2006).

[5] Turner, J., Estrada, H., Kneipp, M., and Razansky, D., "Improved optoacoustic microscopy through three-dimensional spatial impulse response synthetic aperture focusing technique," *Optics letters* **39**(12), 3390–3393 (2014).

[6] Ángel Araque Caballero, M., Rosenthal, A., Gateau, J., Razansky, D., and Ntziachristos, V., "Model-based optoacoustic imaging using focused detector scanning," *Opt. Lett.* **37**, 4080–4082 (Oct 2012).

[7] Deán-Ben, X. L., Estrada, H., Kneipp, M., Turner, J., and Razansky, D., "Three-dimensional modeling of the transducer shape in acoustic resolution optoacoustic microscopy," in [*SPIE BiOS*], 89434V–89434V, International Society for Optics and Photonics (2014).

[8] Strohm, E. M., Moore, M. J., and Kolios, M. C., "High resolution ultrasound and photoacoustic imaging of single cells ‘," *Photoacoustics* (2016).

[9] Chen, S.-L., Xie, Z., Guo, L. J., and Wang, X., "A fiber-optic system for dual-modality photoacoustic microscopy and confocal fluorescence microscopy using miniature components," *Photoacoustics* **1**(2), 30 – 35 (2013).

[10] Ma, R., Söntges, S., Shoham, S., Ntziachristos, V., and Razansky, D., "Fast scanning coaxial optoacoustic microscopy," *Biomedical optics express* **3**(7), 1724 (2012).

[11] Schwarz, M., Omar, M., Buehler, A., Aguirre, J., and Ntziachristos, V., "Implications of ultrasound frequency in optoacoustic mesoscopy of the skin," *Medical Imaging, IEEE Transactions on* **34**(2), 672–677 (2015).

[12] Estrada, H., Turner, J., Kneipp, M., and Razansky, D., "Real-time optoacoustic brain microscopy with hybrid optical and acoustic resolution," *Laser Physics Letters* **11**(4), 045601 (2014).

[13] Cao, R., Kilroy, J. P., Ning, B., Wang, T., Hossack, J. A., and Hu, S., "Multispectral photoacoustic microscopy based on an optical–acoustic objective," *Photoacoustics* **3**(2), 55–59 (2015).

[14] Rosenthal, A., Razansky, D., and Ntziachristos, V., "Fast semi-analytical model-based acoustic inversion for quantitative optoacoustic tomography," *Medical Imaging, IEEE Transactions on* **29**(6), 1275–1285 (2010).

[15] Jensen, J. A., "Field: A program for simulating ultrasound systems," in [*10th Nordicbaltic Conference on Biomedical Imaging*], **4**(1), 351–353, Citeseer (1996).

[16] Estrada, H., Turner, J., Kneipp, M., and Razansky, D., "Real-time optoacoustic brain microscopy with hybrid optical and acoustic resolution," *Laser Physics Letters* **11**(4), 045601 (2014).